

RESEARCH ARTICLE

[View Article Online](#)
[View Journal](#) | [View Issue](#)



Cite this: *RSC Med. Chem.*, 2026, 17, 1155

Exploiting intracellular oncogenic proteins to release cytotoxins

Matthias Schild and Dennis Gillingham *

The success of antibody-drug conjugates has demonstrated the value of targeted delivery strategies for cytotoxic molecules. However, many oncogenic drivers remain inaccessible to antibodies due to their intracellular location, and these drivers are currently mainly addressed using small molecule inhibitors. This work explores repurposing such inhibitors for the intracellular delivery and controlled release of cytotoxic payloads. Using click-to-release chemistry, a pre-targeting strategy was developed where inhibitor-tetrazine conjugates enable selective activation of systemically administered *trans*-cyclooctene (TCO) caged prodrugs. This concept was demonstrated using the epidermal growth factor receptor (EGFR), a key therapeutic target in non-small cell lung cancer. An afatinib-tetrazine conjugate achieved sufficient intracellular retention in EGFR-overexpressing cells to enable toxicity recovery from a TCO-protected monomethyl auristatin E (MMAE) derivative. Successful intracellular targeting and controlled payload release establish a foundation for expanding the scope of targeted drug delivery to previously inaccessible oncogenic drivers.

Received 29th August 2025,
Accepted 11th December 2025

DOI: 10.1039/d5md00764j

rsc.li/medchem

Introduction

Systemically administered chemotherapy and targeted oncology agents have proven highly effective in many types of cancer. Especially with chemotherapeutic agents, however, dose-limiting acute and long-term side effects limit their potential.^{1–4} In recent decades, active or ligand-targeted delivery methods have emerged to overcome toxicity by delivering the payload specifically to the desired site, thereby reducing systemic exposure.^{5,6} A typical approach is to couple an unspecific drug to a ligand that binds tightly with a cancer-associated biomarker. The targeting ligands can vary in composition (*e.g.* there are many cases of small molecules^{7,8} or peptides),^{9–11} but antibody-drug conjugates (ADCs), where antibodies are linked to cytotoxic payloads, are currently the most successful embodiment of the approach.^{12,13}

Upon reaching the intended site, payloads generally require release from their delivery carriers to become therapeutically active, except in certain cases such as with radioligands. This release is commonly facilitated by differences in stimuli between malignant and healthy tissue or through lysosomal cleavage after internalization. While enzymatic cleavage is the most widely used approach, differences in pH or redox environment have also been exploited.¹⁴ Unfortunately, these stimuli are not perfectly

binary; hence an exogenous trigger could be helpful in minimizing premature and off-target release. Light-activation¹⁵ and click-to-release¹⁶ chemistry are the most common options. The click-to-release approach is particularly compelling; here (most commonly) alcohols in allylic positions on *trans*-cyclooctene (TCOs) can be eliminated following an inverse electron demand Diels–Alder (IEDDA)¹⁷ reaction with a tetrazine. By eliminating the need for endogenous release control, click-to-release has opened up a new field of research, with controlled release having been demonstrated using ADCs,^{18,19} peptide-drug conjugates,^{20,21} carbon nanotubes,²² nanoparticles,²³ micelles,^{24–26} supramolecular assembly-based strategies/enzyme-instructed supramolecular self-assembly (EISA),^{27–29} metabolic glycoengineering,³⁰ hydrogels,^{31–33} and small molecules.^{34,35}

Targeted delivery for oncology requires distinguishing characteristics between healthy and cancerous tissue. This differentiation is typically achieved by targeting cancer specific cell surface markers (*i.e.* antibody or peptide targeting), or by exploiting drug activation driven by chemical or physiological differences in the tumor microenvironment.³⁶ Many oncoproteins, however, remain inaccessible to these targeting methods because they are intracellular.³⁷ This work proposes exploiting such intracellular oncogenic proteins for pre-targeting a click-to-release agent (here a tetrazine-bound inhibitor). Subsequent treatment with TCO-caged prodrugs would then trigger an IEDDA/allylic elimination cascade to release the drug. This strategy would have the dual benefit of inhibiting the original

Department of Chemistry, University of Basel, 4056 Basel, Switzerland.
E-mail: dennis.gillingham@unibas.ch



oncoprotein, while also releasing a toxin in response to its presence, which may hinder the emergence of resistance.³⁸ PET tracers based on clinically approved small molecule inhibitors have successfully imaged tumors with specific oncoprotein expression, as demonstrated in human trials for the G12C mutation of Kirsten rat sarcoma gene (KRAS^{G12C})³⁹ and epidermal growth factor receptor (EGFR).⁴⁰ Although cases of using intracellular targets to aid in drug release are rare, recently developed covalent addition/elimination systems are exciting innovations.^{41–44} Here we establish a viable working system for click-to-release activation based on covalent targeting of EGFR (Fig. 1). EGFR ticked all the boxes as a targeting handle since it is frequently mutated and/or overexpressed in malignant tumors,⁴⁵ and has been a major focus of drug development (10 of the 80 FDA-approved kinase

inhibitors target EGFR or the ERBB subfamily), meaning many good inhibitors are available.⁴⁶

Results

Molecular design and target engagement

We settled on the covalent EGFR inhibitor afatinib (**Afa**, see bottom right of Scheme 1, first disclosed in 2008⁴⁷ and approved by the FDA in 2013)⁴⁸ as the targeting ligand⁴⁹ because of its covalent mechanism, and its established track record for integration in bifunctional molecules. For example, **Afa** derivatives have been used to visualize EGFR-expressing tumors in mice⁵⁰ and humans,⁴⁰ and also been used to create bifunctional protein degraders.⁵¹ Based on this prior art, we designed and

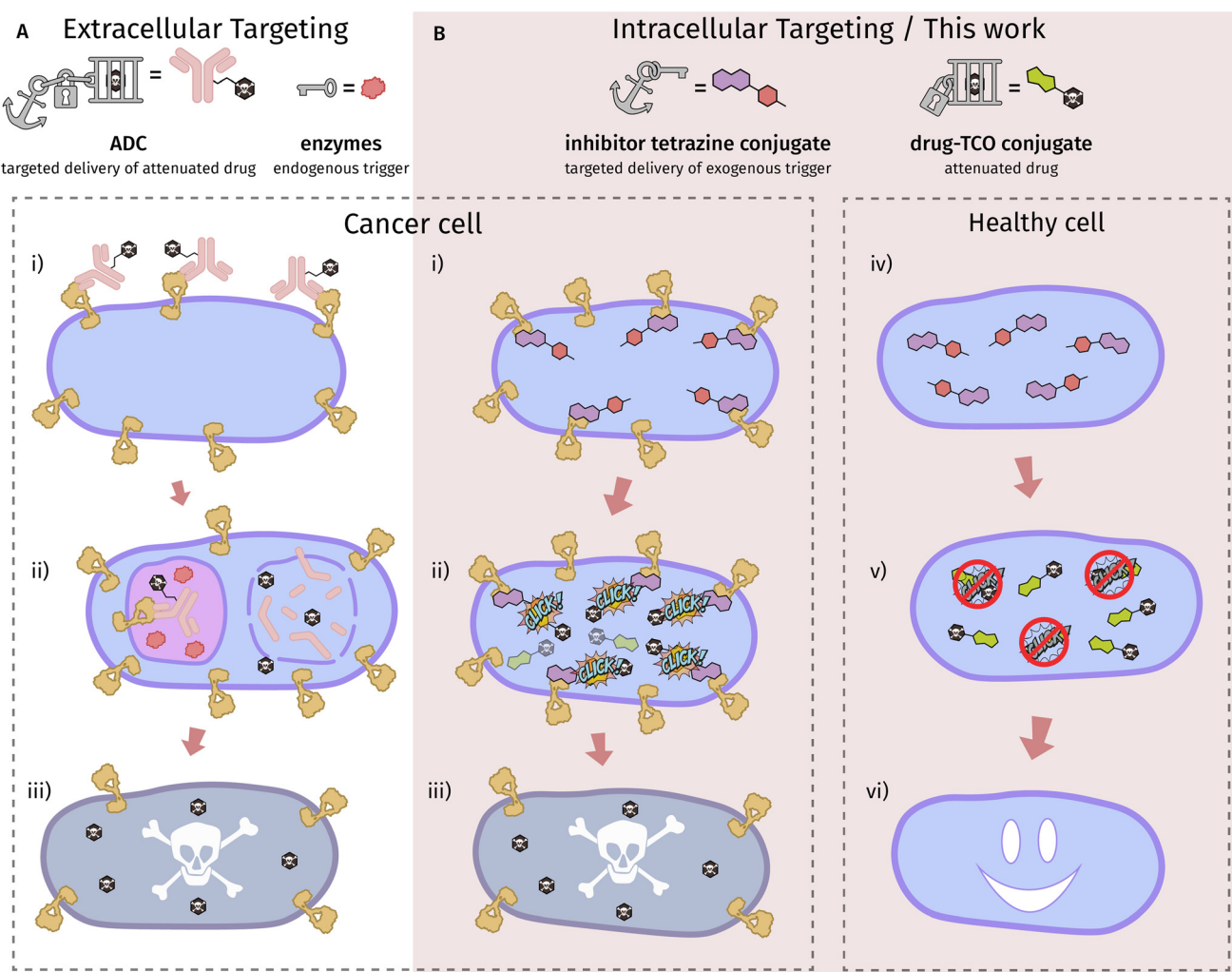
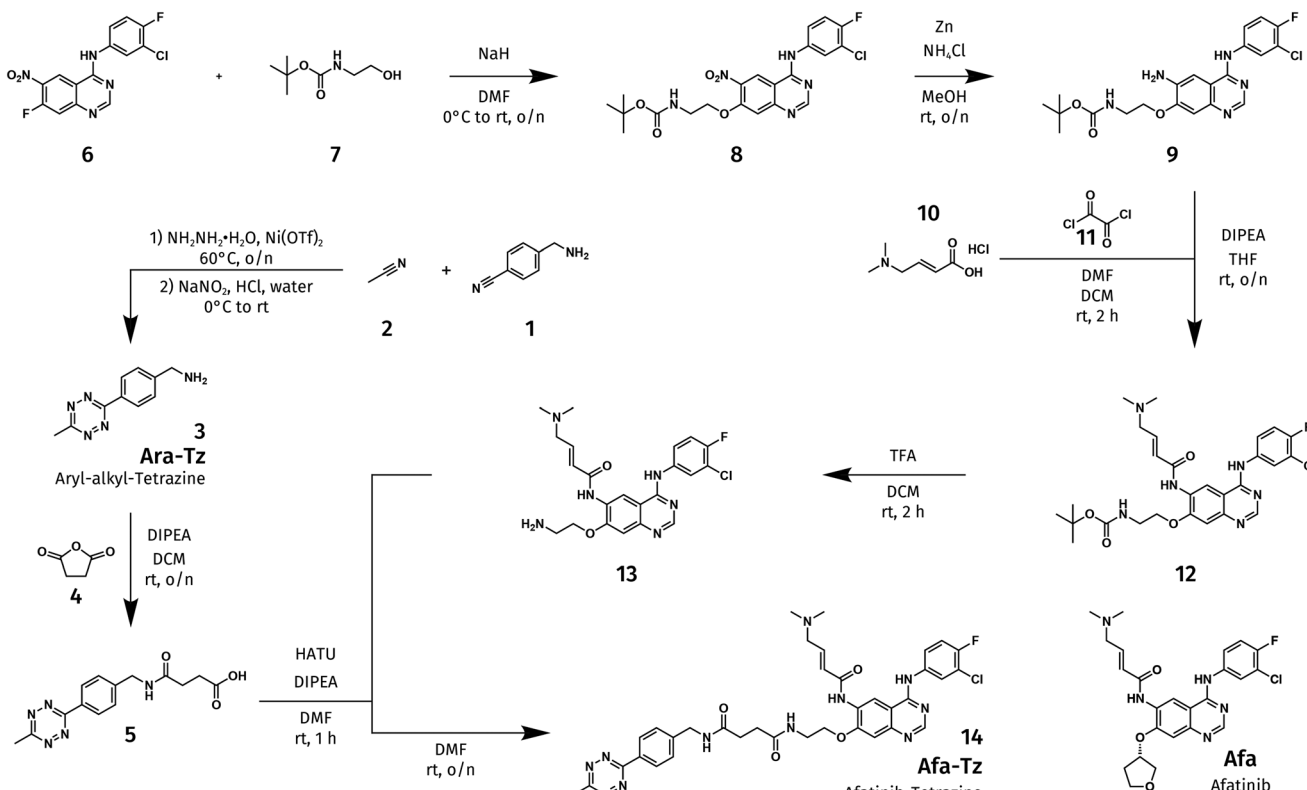


Fig. 1 Concept and design. A. Typical targeted delivery systems such as ADCs exploit extracellular markers to achieve selectivity. The process involves: i) recognition and binding of the ADC to cell surface receptors on cancer cells, ii) internalization of the ADC complex followed by payload release triggered by endogenous enzymes within the lysosome, and iii) subsequent cell death induced by the liberated cytotoxic agent. B. Our approach leverages a two-part system with sequential administration where overexpressed intracellular targets guide the release of toxins. In a cancer cell: i) an inhibitor-tetrazine conjugate functions as a targeted exogenous trigger which binds and accumulates at its intracellular target, ii) a subsequently administered prodrug attenuated through TCO-protection undergoes click-to-release with the pre-localized tetrazine moieties, iii) activating the payload and inducing cell death. In contrast, iv) the tetrazine has no binding site in a healthy cell and therefore cannot lead to v) click-to-release reaction activation, vi) sparing healthy cells from toxicity.



Scheme 1 Synthesis of a version of afatinib bearing a tetrazine (Afa-Tz). Experimental details can be found in the SI.

synthesized a tetrazine bearing version of **Afa** (**Afa-Tz**, Scheme 1) where the linker connecting the tetrazine is installed at the position of the tetrahydrofuran ring in **Afa**. For the tetrazine, we selected the methyl/aryl

substituted derivative (synthesis described in SI) because it is a workhorse structure in IEDDA bioconjugation⁵² and has even been used in phase I clinical trials for click-to-release activation.⁵³

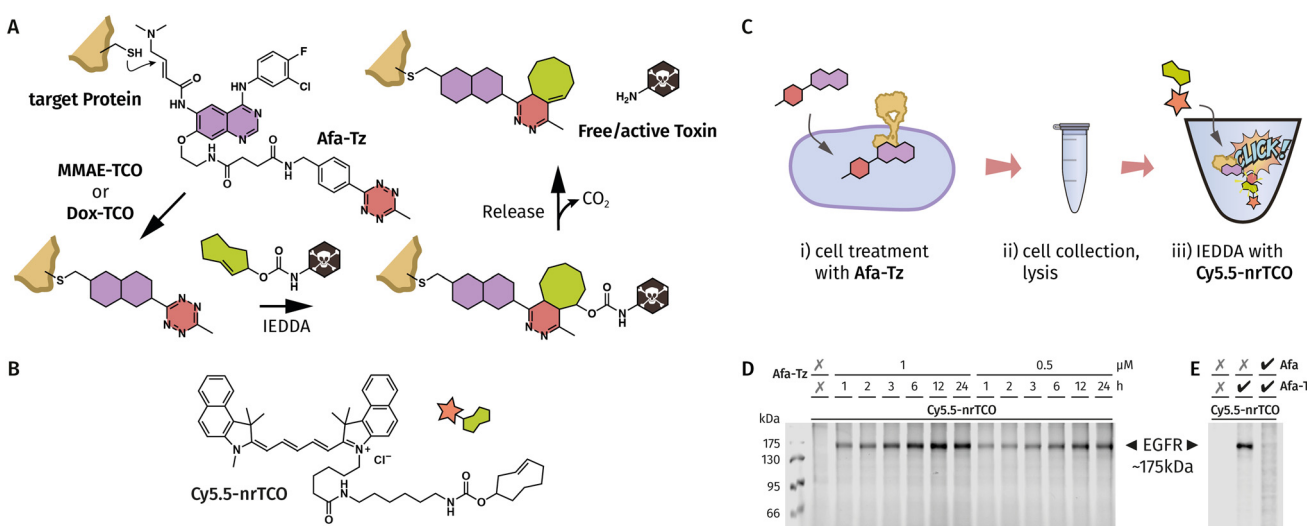


Fig. 2 Characterization of afatinib-tetrazine (Afa-Tz) binding to EGFR. A. Chemical reactions involved in toxin release. B. Structure of the non-releasing fluorophore used to characterize EGFR targeting. C. i) In-cell covalent labelling of EGFR by Afa-Tz followed by ii) collection and lysis of treated cells, iii) click reaction with Cy5.5-nrTCO and separation on PAGE for in-gel fluorescence detection. D. A431 cells overexpressing EGFR treated with Afa-Tz are lysed, treated with Cy5.5-nrTCO, separated using PAGE and visualized at 700 nm. Selective binding can be seen at the expected weight of EGFR. E. Same experiment as in D with additional pre-treatment with parent inhibitor Afa (lane 3) which blocks the active site of EGFR and leads to disappearance of labelled band, demonstrating selectivity.



Before performing toxin release (Fig. 2A), we first needed to validate EGFR engagement and target selectivity with the **Afa-Tz** probe, as well as its proficiency at IEDDA. We therefore prepared a non-releasing TCO derivative bearing a Cy5.5 dye (**Cy5.5-nrTCO**, Fig. 2B), and used it to examine covalent targets of **Afa-Tz** in in-gel fluorescence assays (Fig. 2C–E). Specifically, the epidermoid carcinoma cells A431 (which are high in EGFR)^{47,54} were first treated with **Afa-Tz** for the appropriate time and then lysed, **Cy5.5-nrTCO** was then added before loading the samples on a gel (Fig. 2C). The data indicate (Fig. 2D) that **Afa-Tz** labels EGFR at both 1 μ M and 500 nM, with optimal labelling at 12 h, although a robust signal is already seen at 1 h. Importantly, if we pre-treat the cells with the parent inhibitor **Afa**, the labelling with **Afa-Tz** is blocked and no fluorescent band is observed (Fig. 2E). EGFR western blotting (Fig. 5A) confirms the identity of the labelled band, and the lack of any other fluorescent bands in the complete gels (see Fig. S5 and S6) speaks to highly selective labelling. An interesting side-note is that when we block EGFR with **Afa**,

there is a noticeable increase in off-target labelling (see last column of Fig. 2E). This can be rationalized by considering that when EGFR is not available as a rapid sink for **Afa-Tz**, its increased effective concentration promotes off-target, lower affinity binding events.

Click-to-release of the topoisomerase poison doxorubicin (Dox) and tubulin poison monomethylauristatin E (MMAE)

As our initial TCO-caged drug candidates we selected two well-studied cytotoxins: **Dox** and **MMAE**. **Dox** (Fig. 3A) is a topoisomerase poison that is widely used as a chemotherapeutic agent,⁵⁵ and whose known toxicity profile continues to drive efforts to develop safer delivery methods.⁵⁶ It was among the first drugs demonstrated in click-to-release systems¹⁶ and now frequently serves as a benchmark for evaluating novel drug activation strategies^{57,58} and other

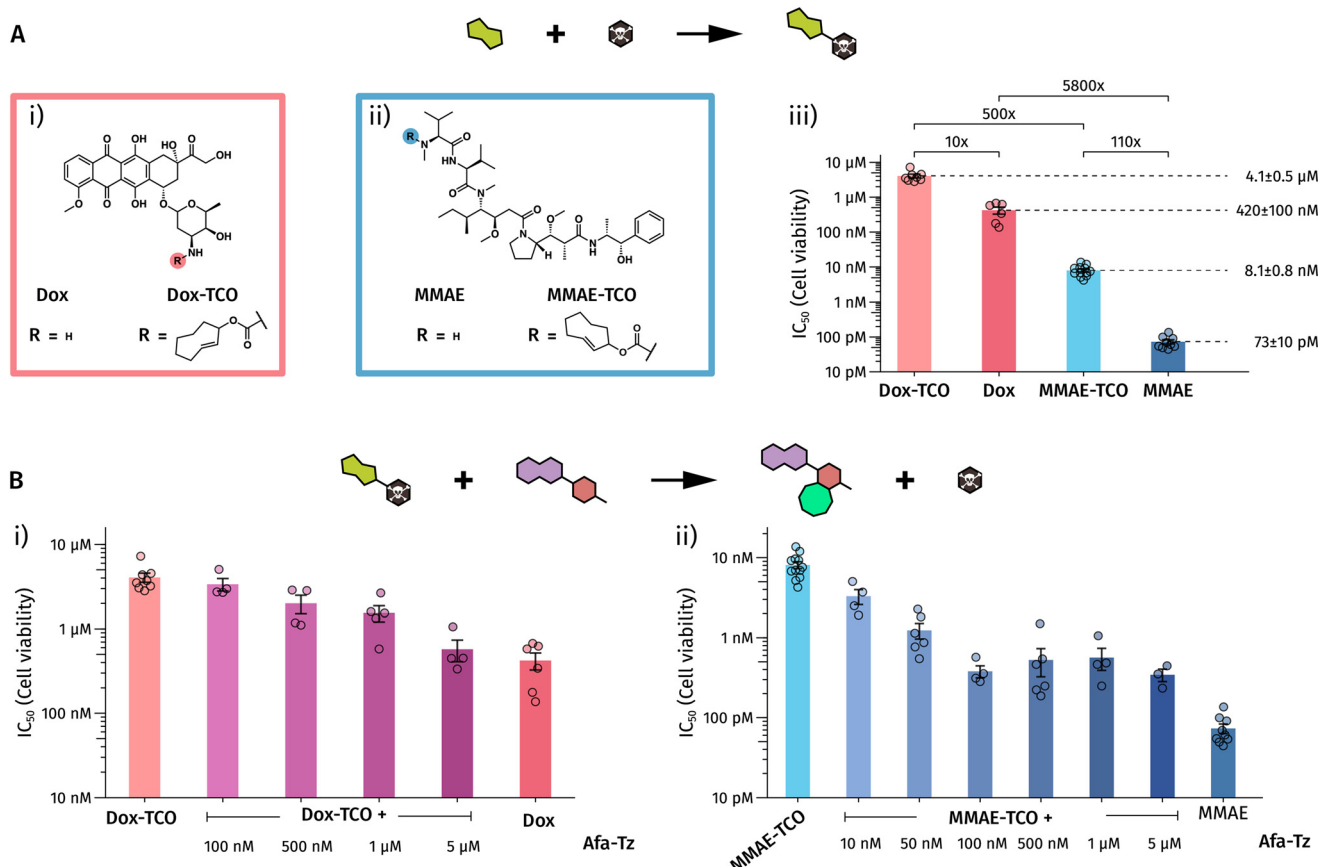


Fig. 3 TCO protection attenuates drug toxicity and tetrazine-mediated activation restores potency. **A.** Structures and characterization of parent cytotoxins and their TCO-caged derivatives i) **Dox** and ii) **MMAE**. **iii)** Comparison of cell viability shows TCO caging attenuates Dox toxicity approximately 10-fold, while MMAE shows greater attenuation at 110-fold. Notably, MMAE is significantly more potent than Dox as a parent compound (5800-fold). **B.** Co-incubation of IEDDA partners demonstrates dose-dependent restoration of drug activity. i) **Dox-TCO** dilutions co-incubated with fixed concentrations of **Afa-Tz** show progressive toxicity recovery approaching that of parent **Dox**. ii) Experiments with **MMAE-TCO** demonstrate more efficient recovery, with significant activity restoration already at 10 nM **Afa-Tz** and reaching maximum effect at just 100 nM, beyond which additional tetrazine provides no further benefit. Cell viability assays performed in A431 cells using resazurin at 72 h. Data points represent independent biological experiments, bars and error bars indicate mean and SEM, respectively.



papers citing.¹⁶ **MMAE** (Fig. 3A) is a synthetic derivative of the tubulin poison Dolastatin,⁵⁹ and can only be used as a therapeutic when conjugated with an antibody due to its high systemic toxicity.⁶⁰ The synthesis of caged versions of these agents, **Dox-TCO** and **MMAE-TCO** followed established protocols^{57,61} and proceeded without event (detailed synthesis in the SI). We first evaluated the impact of TCO caging on the cytotoxic potency of both drugs independent of EGFR-targeting effects. We did this by measuring cell viability changes in A431 cells upon click-to-release reactions with the activating tetrazine, **Afa-Tz**.

Dox-TCO displayed a 10-fold increase in IC_{50} compared to free **Dox** (Fig. 3A(iii); tabulated data for cell viability experiments can be found in the SI), a relatively modest attenuation. This raised concerns that the inherent background toxicity of **Dox-TCO** might overshadow potential benefits from selective activation – a concern highlighted by Morese *et al.*⁴¹ in their study of covalent ligand-directed release of 5-fluorouracil upon EGFR binding. In contrast, **MMAE-TCO** exhibited a substantial 111-fold increase in IC_{50} over free **MMAE** (8.1 ± 0.8 nM vs. 73 ± 10 pM), indicating a far greater attenuation of toxicity and thus a larger therapeutic window for activation. In parallel with these efforts we also examined the change in IC_{50} caused by the chemical changes we introduced on **Afa** to make **Afa-Tz**. Importantly, the **Afa-Tz** IC_{50} is 25 ± 9 μ M (see Fig. S2), which is significantly higher than the **Dox-TCO** and **MMAE-TCO** IC_{50} s, meaning there is low risk that effects below an IC_{50} of 10μ M have any connection to EGFR inhibition. Although **Afa-Tz** toxicity arising from EGFR inhibition is therapeutically desirable, for quantitatively studying the pre-targeting

effect it is ideal to have a window where the pre-targeting driven toxicity is clearly differentiated from inhibition.

We next performed co-incubation experiments to evaluate re-activation efficiency of caged drugs by treating cells simultaneously with **Afa-Tz** and the respective TCO-caged drug (see Fig. 3B(i)). For **Dox-TCO**, using 5μ M **Afa-Tz** restored cytotoxicity to levels approaching free **Dox** (IC_{50} 420 ± 100 nM). Even at lower **Afa-Tz** concentrations (1μ M), substantial cytotoxic enhancement was observed, clearly confirming the click-to-release activation. **MMAE-TCO** activation proved more effective: co-incubation with 5μ M **Afa-Tz** enhanced toxicity nearly 30-fold compared to **MMAE-TCO** alone (see Fig. 3B(ii)). At 1μ M **Afa-Tz**, activation remained strong and consistent down to 100 nM **MMAE-TCO**, underscoring **MMAE**'s sensitivity to the click-to-release mechanism.

In vivo pre-targeting would rely on a subject's circulatory system to distribute the pre-targeting agent, where it would be transiently exposed to all tissues and cells, but gradually accumulate in the target tissue because that event is irreversible.⁶² To simulate these conditions in cell culture we used washing steps after a specified incubation time. Specifically, after seeding, cells were treated (*i.e.* pre-targeted) with **Afa-Tz** and incubated for a defined period (data in Fig. 2D led us to select 1–6 h), followed by multiple medium changes to remove unbound **Afa-Tz**. Subsequently, TCO-caged drug dilutions were added and the standard viability assay was run. Initial pre-targeting experiments with **Dox-TCO** (1μ M **Afa-Tz** for 1 h, followed by extensive washing) failed to demonstrate enhanced cytotoxicity compared to **Dox-TCO** alone. Increasing incubation times (up to 6 h) or **Afa-Tz** concentrations (5μ M) also yielded no improvement, suggesting that pre-targeting efficacy with **Dox-TCO** is limited

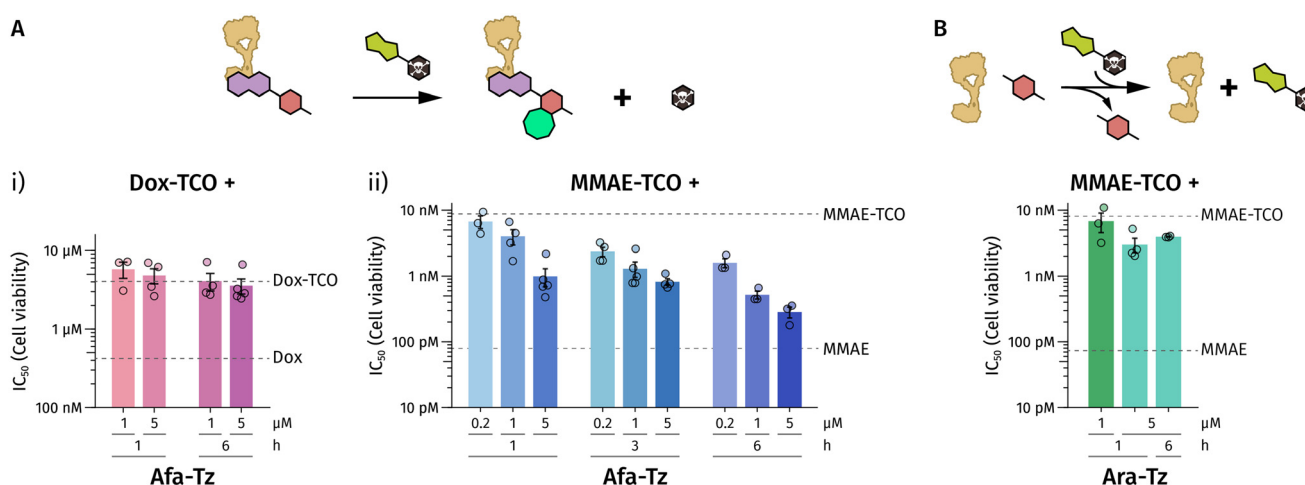


Fig. 4 Pre-targeting with **Afa-Tz** enables activation of **MMAE-TCO** but not **Dox-TCO**. A. Pre-targeting strategy: A431 cells are first incubated with **Afa-Tz**, washed, and then exposed to TCO-protected drugs. i) Pre-targeting in A431 cells with **Afa-Tz** at various concentrations and incubation times fails to effectively activate **Dox-TCO**, showing no recovery toward parent **Dox** potency. ii) The same pre-targeting approach with **MMAE-TCO** demonstrates both concentration- and time-dependent activation, with longer incubation times and higher concentration treatments yielding greater toxicity recovery. B. When using a non-targeted tetrazine (**Ara-Tz**) lacking EGFR-binding capability, **MMAE-TCO** shows only minimal activation. Cell viability assays performed in A431 cells using resazurin at 72 h. Data points represent independent biological experiments, bars and error bars indicate mean and SEM, respectively. Average IC_{50} values of parent compound and TCO-caged compounds are indicated by horizontal dashed lines representing means.



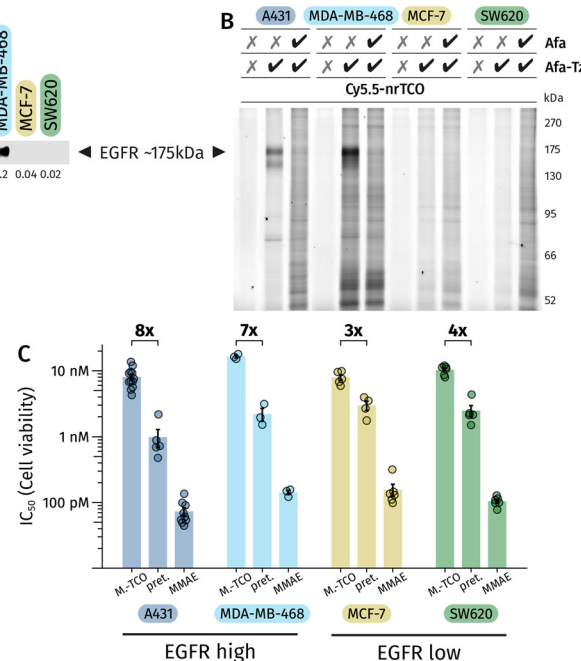


Fig. 5 Pre-targeting efficacy correlates with EGFR expression across cell lines. **A.** Western blot analysis reveals high EGFR expression in A431 and MDA-MB-468 and low expression in MCF-7 and SW620. Values from band integration normalized to total protein stain. **B.** In-gel fluorescence experiment (as in Fig. 2D) across the cell line panel. Strong bands at \sim 175 kDa from **Afa-Tz** treatment are observed only in EGFR-high cell lines and can be blocked by pretreatment with **Afa** indicating selective EGFR targeting. **C.** Cell viability comparison across cell lines showing toxicities for parent drug **MMAE**, pro-drug **MMAE-TCO**, and pre-targeting with **Afa-Tz** (5 μ M, 1 h) followed by **MMAE-TCO** treatment. EGFR-high cell lines demonstrate stronger toxicity recovery (8-fold and 7-fold enhancement) compared to EGFR-low cell lines (3-fold and 4-fold enhancement), though background activation is observed in all cases. Data points represent independent biological experiments, bars and error bars indicate mean and SEM, respectively.

by insufficient tetrazine retention or inadequate potency or both (see Fig. 4A(i)). Given these limitations, we shifted focus to **MMAE-TCO**, hoping that its higher potency would improve outcomes. Indeed, pre-targeting experiments with **MMAE-TCO** (5 μ M **Afa-Tz**, 1 h) successfully demonstrated toxicity recovery, reducing the IC_{50} from 8.1 ± 0.8 nM (**MMAE-TCO** alone) to 1.0 ± 0.3 nM. Optimization of pre-targeting conditions further enhanced recovery, reaching an IC_{50} as low as 280 ± 50 pM (5 μ M, 6 h; see Fig. 4A(ii)).

Our pre-targeting strategy relies on tetrazine retention through covalent binding to EGFR. Hence as a control for nonspecific retention, we performed pre-targeting assays with a minimal aryl-alkyl-tetrazine (**Ara-Tz**, see Scheme 1) under identical conditions to those used for **Afa-Tz**. These experiments confirmed that toxicity recovery depended primarily on specific EGFR engagement by **Afa-Tz**, although there does seem to be some background retention as **Ara-Tz** treatment leads to a slight increase in **MMAE-TCO** toxicity (see Fig. 4B). Co-incubation of **MMAE-TCO** with **Afa-Tz** or **Ara-Tz** (see Fig. 3B(ii) and S3), showed similar toxicity

recovery (approximately 20-fold), confirming that the **Tz** incorporated in **Ara-Tz** is as efficient as the **Afa-Tz** in the IEDDA reaction. Under our initial conditions (5 μ M and 1 h, see Fig. 4B), **Ara-Tz** pre-targeting showed only a two-fold toxicity increase relative to **MMAE-TCO**, indicating good (but incomplete) washout. In contrast, **Afa-Tz** demonstrated superior retention with an eight-fold toxicity increase (see Fig. 4A(ii)). At lower concentrations (1 μ M and 1 h), both compounds showed similar but low toxicity recovery, suggesting that any observed activation by **Afa-Tz** at these lower concentrations likely resulted from unspecific retention rather than selective EGFR binding. Unselective cellular retention is a well-documented challenge in fluorescent imaging^{63,64} where background fluorescence can persist after multiple washes over extended periods.^{65–67} Nevertheless, the correlation between reactivation and EGFR expression supports EGFR-dependent click-to-release.

EGFR dependence

To examine the extent of EGFR dependency, we performed pre-targeting experiments on a panel of cell lines differing in EGFR expression: EGFR-positive A431 and MDA-MB-468, and EGFR-negative MCF-7 and SW620. Western blotting confirmed strong EGFR expression in A431 and MDA-MB-468, and minimal expression in MCF-7 and SW620 (Fig. 5A). Consistent with these expression patterns, target engagement assays showed robust **Afa-Tz** binding exclusively in EGFR-positive cells (Fig. 5B). Since **Afa** is a pan-ERBB inhibitor, the negative control cell lines should also express low levels of HER2, HER3, and HER4, and since we see no off-target bands in the target engagement assay, we can conclude that covalent targeting of other related ERBB proteins is not a confounding factor.

Having established the extent of covalent binding of **Afa-Tz** in the cell line panel, experiments were conducted to assess the various toxicities induced by this system. Initial measurements focused on baseline toxicities of **MMAE** and the protected drug **MMAE-TCO**. As shown in Fig. 5C, distinct toxicity profiles emerged across the cell lines. In A431, **MMAE** displayed an IC_{50} of 73 ± 10 pM, while **MMAE-TCO** showed reduced toxicity with an IC_{50} of 8.1 ± 0.8 nM, representing a 111-fold reduction. Similar fold-changes in toxicity were observed in MDA-MB-468 (115-fold) and SW620 (98-fold), though at higher absolute IC_{50} values. MDA-MB-468 exhibited IC_{50} values of 143 ± 11 pM for **MMAE** and $16\,500 \pm 800$ pM for **MMAE-TCO**, while SW620 showed IC_{50} values of 105 ± 7 pM for **MMAE** and $10\,300 \pm 700$ pM for **MMAE-TCO**. MCF-7 cells showed a notably different pattern, with **MMAE-TCO** maintaining similar toxicity ($IC_{50} = 7900 \pm 800$ pM) to other cell lines, but **MMAE** showing reduced potency ($IC_{50} = 160 \pm 30$ pM), resulting in only a 49-fold reduction. In all cases, **MMAE-TCO** co-incubated with 5 μ M **Afa-Tz** was approximately 5 times less toxic than **MMAE** itself, with the relative shift between cell lines remaining consistent.

As toxicity recovery could be shown in all cell lines from co-incubating **Afa-Tz** and **MMAE-TCO**, we next pre-targeted



the **Afa-Tz** to EGFR before treating with **MMAE-TCO**. As previously shown, A431 exhibited an 8-fold increase in toxicity under our standard pre-targeting conditions (5 μ M for 1 h) with **Afa-Tz** (Fig. 4A(ii)). Applying these conditions in MDA-MB-468 led to a very similar 7-fold increase in toxicity. Although some toxicity recovery was observed in the negative control cell lines (see EGFR low cells in Fig. 5C), we could always clearly distinguish the EGFR effect.

Discussion

Most current click-to-release drug activation systems rely primarily on specific cell surface receptors or specific biomarkers in the tumor stroma to achieve targeting. In contrast, our approach uniquely exploits the stoichiometric binding of a tetrazine-conjugated ligand (**Afa-Tz**) to individual EGFR molecules inside the cell. While offering new opportunities for selectivity, our approach limits the maximum achievable drug release to the number of available EGFR binding sites per cell. Consequently, achieving therapeutically effective drug concentrations *via* this mechanism depends on the potency of the selected cytotoxic payload and the overexpression of the targeting receptor. Calculations indicate⁶⁸ that even under ideal conditions, EGFR-targeted release of a drug like **Dox** would generate intracellular concentrations approaching only 1 μ M. Given the moderate potency of **Dox** (IC_{50} around 0.42 μ M in A431 cells), our system was insufficient to achieve observable therapeutic effects (top pathway in Fig. 6). This highlights the necessity of using more potent cytotoxins to fully exploit

the potential of stoichiometric click-to-release strategies (represented graphically in Fig. 6). To address this, we turned to **MMAE**, a highly potent tubulin inhibitor widely utilized as an ADC payload. **MMAE** is several orders of magnitude more toxic than **Dox**, making it an ideal candidate to overcome stoichiometric limitations inherent in EGFR-targeted click-to-release. Indeed, our results confirmed that TCO-caged **MMAE** exhibited significantly greater potency and therapeutic window upon activation compared to **Dox-TCO**.

Our caged constructs showed only moderate toxicity attenuation, which would result in substantial systemic toxicity – a key limitation to practical applications. However, this is a known problem in the field and others are actively investigating linker chemistry,⁶⁹ release chemistry, and attachment position to improve this point.^{70,71} A more systematic investigation into drug “cage-ability” – with the goal of developing caged payloads that are substantially less toxic in their inactivated state – would benefit the field as a whole, as improved caging strategies can be directly integrated into any click-to-release platform.

Importantly, click-to-release activation of **MMAE-TCO** with **Afa-Tz** was successful even at low tetrazine concentrations, underscoring the sensitivity of **MMAE** to this activation mechanism. Pre-targeting assays further validated that effective drug activation was dependent on EGFR expression, although nonspecific cellular retention of the activating tetrazine remains a challenge requiring optimization. Importantly, our careful comparative analysis between two separate payloads across several cell lines gives a roadmap for future designs. Specifically, we now understand that complete deactivation of

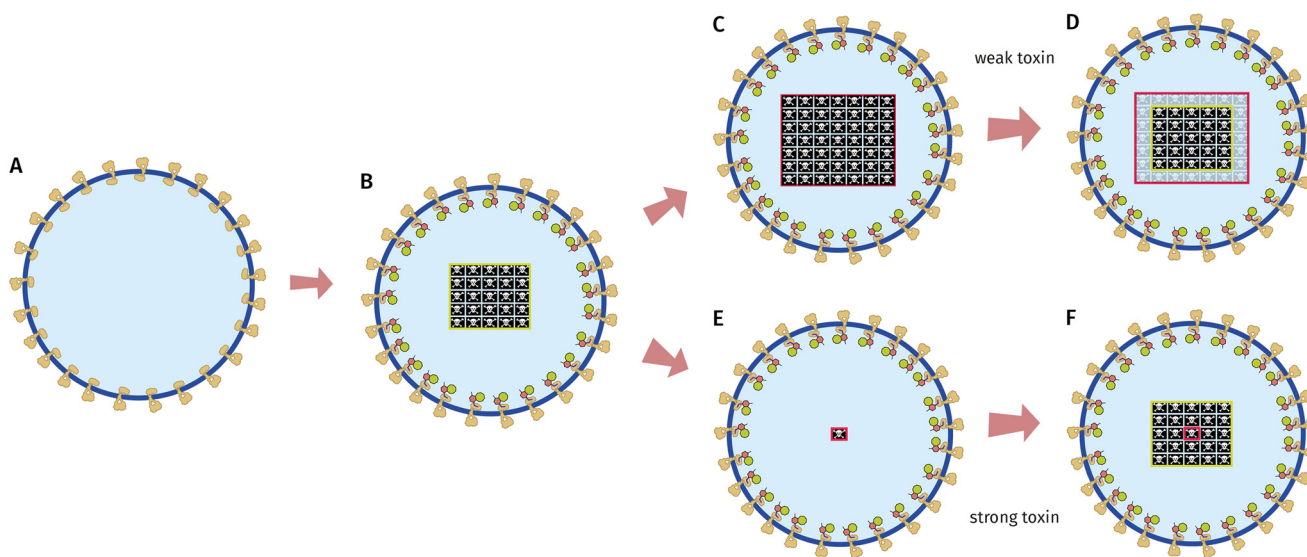


Fig. 6 Potent toxins are essential for effective pre-targeting strategy. A. Cancer cell with EGFR receptors expressed on the surface. B. **Afa-Tz** binds to EGFR receptors and accumulates in the cell, but after washout cannot exceed the concentration limited by available receptor sites. Pre-targeted **Afa-Tz** is at maximum able to activate a stoichiometric amount of prodrug (yellow square) relative to the number of EGFR receptors. Upper pathway, weak toxin scenario: C. A weak toxin (like **Dox**) requires many molecules per cell (red square) to achieve cell death. D. When activated by pre-targeted tetrazine, the concentration of released active drug (yellow square) is insufficient to reach lethal threshold (red square), resulting in limited efficacy. Lower pathway, strong toxin scenario: E. A potent toxin (like **MMAE**) requires very few molecules (red square) per cell to achieve cell death. F. Even the small amount (yellow square) activated by the limited pre-targeted tetrazine is sufficient to kill the cell effectively.



the caged pro-drug is important and that the bulk cellular retention of the pre-targeting agent should be quantified. The availability of clinically validated covalent ligands for important oncology and immunology targets is expanding rapidly, hence an exciting future prospect would be to repurpose some of these ligand/oncoprotein conjugates to drive pre-targeting. Moving beyond EGFR is also an important future direction, as is the possibility of achieving catalysis by using reversible covalent ligands⁷² (catalysis in receptor) or delivering molecular glue or PROTAC degraders (catalytic loss of target) or both.^{73,74} Related concepts are already being explored in the ADC world.^{75,76}

Overall, our study demonstrates the critical importance of cytotoxic potency, target expression, and selective retention in designing effective pre-targeted drug delivery systems. MMAE's superior potency and robust activation profile position it as particularly suited to EGFR-targeted click-to-release approaches, highlighting a promising pathway for developing more effective and selective cancer therapies. Although targeting intracellular cancer-specific targets will likely not have the same target scope as extracellular ones, there are clear potential use cases, such as in G12C mutations of KRAS,^{77,78} in cysteine mutants of p53,⁷⁹ or highly overexpressed kinases (like EGFR selected here) that contain ligandable cysteines.

Author contributions

M. S. conceptualized the study, developed and performed experiments, analyzed and visualized data and wrote the original draft and edited and revised the manuscript. D. G. initiated and conceptualized the study, supervised the project, and edited and revised the manuscript.

Conflicts of interest

There are no conflicts to declare.

Data availability

The data supporting this article have been included as part of the supplementary information (SI).

Supplementary information: the SI includes detailed synthesis protocols and associated characterization data, uncropped gels related to images in the figures, detailed biological protocols including IC₅₀ determinations. See DOI: <https://doi.org/10.1039/d5md00764j>.

Acknowledgements

We would like to thank Dr. Seemon Coomar and Dr. Angel Cores for fruitful discussions as well as Dr. Basilius Sauter for input on data analysis and visualization. We are grateful to Minqi Pan for assistance with NMR spectroscopy and HRMS measurements and Hortense Danteville for contributions to the synthesis. The University of Basel and the European Research Council (Horizon 2020, ExploDProteins, 866345) are gratefully acknowledged for supporting this work.

References

- I. Raber and A. Asnani, Cardioprotection in cancer therapy: novel insights with anthracyclines, *Cardiovasc. Res.*, 2019, **115**, 915–921.
- N. M. Kuderer, A. Desai, M. B. Lustberg and G. H. Lyman, Mitigating acute chemotherapy-associated adverse events in patients with cancer, *Nat. Rev. Clin. Oncol.*, 2022, **19**, 681–697.
- M. B. Lustberg, N. M. Kuderer, A. Desai, C. Bergerot and G. H. Lyman, Mitigating long-term and delayed adverse events associated with cancer treatment: implications for survivorship, *Nat. Rev. Clin. Oncol.*, 2023, **20**, 527–542.
- R. Juthani, S. Punatar and I. Mittra, New light on chemotherapy toxicity and its prevention, *BJC Rep.*, 2024, **2**, 41.
- Z. Zhao, A. Ukidve, J. Kim and S. Mitragotri, Targeting Strategies for Tissue-Specific Drug Delivery, *Cell*, 2020, **181**, 151–167.
- M. Srinivasarao and P. S. Low, Ligand-Targeted Drug Delivery, *Chem. Rev.*, 2017, **117**, 12133–12164.
- L. Wang, M. Tran, E. D'Este, J. Roberti, B. Koch, L. Xue and K. Johnsson, A general strategy to develop cell permeable and fluorogenic probes for multicolour nanoscopy, *Nat. Chem.*, 2020, **12**, 165–172.
- T. K. Patel, N. Adhikari, S. A. Amin, S. Biswas, T. Jha and B. Ghosh, Small molecule drug conjugates (SMDCs): an emerging strategy for anticancer drug design and discovery, *New J. Chem.*, 2021, **45**, 5291–5321.
- V. P. Chavda, H. K. Solanki, M. Davidson, V. Apostolopoulos and J. Bojarska, Peptide-Drug Conjugates: A New Hope for Cancer Management, *Molecules*, 2022, **27**, 7232.
- T. T. Dean, J. Jelú-Reyes, A. L. C. Allen and T. W. Moore, Peptide-Drug Conjugates: An Emerging Direction for the Next Generation of Peptide Therapeutics, *J. Med. Chem.*, 2024, **67**, 1641–1661.
- B. Zhang, M. Wang, L. Sun, J. Liu, L. Yin, M. Xia, L. Zhang, X. Liu and Y. Cheng, Recent Advances in Targeted Cancer Therapy: Are PDCs the Next Generation of ADCs?, *J. Med. Chem.*, 2024, **67**, 11469–11487.
- C. Dumontet, J. M. Reichert, P. D. Senter, J. M. Lambert and A. Beck, Antibody-drug conjugates come of age in oncology, *Nat. Rev. Drug Discovery*, 2023, **22**, 641–661.
- Z. Fu, S. Li, S. Han, C. Shi and Y. Zhang, Antibody drug conjugate: the “biological missile” for targeted cancer therapy, *Signal Transduction Targeted Ther.*, 2022, **7**, 93.
- J. D. Bargh, A. Isidro-Llobet, J. S. Parker and D. R. Spring, Cleavable linkers in antibody-drug conjugates, *Chem. Soc. Rev.*, 2019, **48**, 4361–4374.
- E. Maurits, M. J. v. d. Graaff, S. Maiorana, D. P. A. Wander, P. M. Dekker, S. Y. v. d. Zanden, B. I. Florea, J. J. C. Neefjes, H. S. Overkleft and S. I. v. Kasteren, Immunoproteasome Inhibitor-Doxorubicin Conjugates Target Multiple Myeloma Cells and Release Doxorubicin upon Low-Dose Photon Irradiation, *J. Am. Chem. Soc.*, 2020, **142**, 7250–7253.
- R. M. Versteegen, R. Rossin, W. t. Hoeve, H. M. Janssen and M. S. Robillard, Click to Release: Instantaneous Doxorubicin



Elimination upon Tetrazine Ligation, *Angew. Chem., Int. Ed.*, 2013, **52**, 14112–14116.

17 M. L. Blackman, M. Royzen and J. M. Fox, Tetrazine Ligation: Fast Bioconjugation Based on Inverse-Electron-Demand Diels–Alder Reactivity, *J. Am. Chem. Soc.*, 2008, **130**, 13518–13519.

18 R. Rossin, R. M. Versteegen, J. Wu, A. Khasanov, H. J. Wessels, E. J. Steenbergen, W. ten Hoeve, H. M. Janssen, A. H. A. M. van Onzen, P. J. Hudson and M. S. Robillard, Chemically triggered drug release from an antibody-drug conjugate leads to potent antitumour activity in mice, *Nat. Commun.*, 2018, **9**, 1484.

19 R. Rossin, S. M. J. v. Duijnhoven, W. t. Hoeve, H. M. Janssen, L. H. J. Kleijn, F. J. M. Hoeben, R. M. Versteegen and M. S. Robillard, Triggered Drug Release from an Antibody–Drug Conjugate Using Fast “Click-to-Release” Chemistry in Mice, *Bioconjugate Chem.*, 2016, **27**, 1697–1706.

20 X. He, J. Li, X. Liang, W. Mao, X. Deng, M. Qin, H. Su and H. Wu, An all-in-one tetrazine reagent for cysteine-selective labeling and bioorthogonal activatable prodrug construction, *Nat. Commun.*, 2024, **15**, 2831.

21 M. Chang, F. Gao, D. Pontigon, G. Gnawali, H. Xu and W. Wang, Bioorthogonal PROTAC Prodrugs Enabled by On-Target Activation, *J. Am. Chem. Soc.*, 2023, **145**, 14155–14163.

22 H. Li, J. Conde, A. Guerreiro and G. J. L. Bernardes, Tetrazine Carbon Nanotubes for Pretargeted In Vivo “Click-to-Release” Bioorthogonal Tumour Imaging, *Angew. Chem., Int. Ed.*, 2020, **59**, 16023–16032.

23 I. Khan, P. F. Agris, M. V. Yigit and M. Royzen, In situ activation of a doxorubicin prodrug using imaging-capable nanoparticles, *Chem. Commun.*, 2016, **52**, 6174–6177.

24 F. Suehiro, S. Fujii and T. Nishimura, Bioorthogonal micellar nanoreactors for prodrug cancer therapy using an inverse-electron-demand Diels–Alder reaction, *Chem. Commun.*, 2022, **58**, 7026–7029.

25 L. Zuo, J. Ding, C. Li, F. Lin, P. R. Chen, P. Wang, G. Lu, J. Zhang, L.-L. Huang and H.-Y. Xie, Coordinating bioorthogonal reactions with two tumor-microenvironment-responsive nanovehicles for spatiotemporally controlled prodrug activation, *Chem. Sci.*, 2020, **11**, 2155–2160.

26 X. Xie, B. Li, J. Wang, C. Zhan, Y. Huang, F. Zeng and S. Wu, Bioorthogonal Nanosystem for Near-Infrared Fluorescence Imaging and Prodrug Activation in Mouse Model, *ACS Mater. Lett.*, 2019, **1**, 549–557.

27 Q. Yao, F. Lin, X. Fan, Y. Wang, Y. Liu, Z. Liu, X. Jiang, P. R. Chen and Y. Gao, Synergistic enzymatic and bioorthogonal reactions for selective prodrug activation in living systems, *Nat. Commun.*, 2018, **9**, 5032.

28 C. Wu, J. Xie, Q. Yao, Y. Song, G. Yang, J. Zhao, R. Zhang, T. Wang, X. Jiang, X. Cai and Y. Gao, Intrahippocampal Supramolecular Assemblies Directed Bioorthogonal Liberation of Neurotransmitters to Suppress Seizures in Freely Moving Mice, *Adv. Mater.*, 2024, **36**, e2314310.

29 Q. Yao, S. Gao, C. Wu, T. Lin and Y. Gao, Enzymatic non-covalent synthesis of supramolecular assemblies as a general platform for bioorthogonal prodrugs activation to combat drug resistance, *Biomaterials*, 2021, **277**, 121119.

30 M. M. A. Mity, M. L. Dallas, S. Y. Boateng, F. Greco and H. M. I. Osborn, Selective activation of prodrugs in breast cancer using metabolic glycoengineering and the tetrazine ligation bioorthogonal reaction, *Bioorg. Chem.*, 2024, **147**, 107304.

31 J. M. M. Oneto, I. Khan, L. Seebald and M. Royzen, In Vivo Bioorthogonal Chemistry Enables Local Hydrogel and Systemic Pro-Drug To Treat Soft Tissue Sarcoma, *ACS Cent. Sci.*, 2016, **2**, 476–482.

32 M. Czuban, S. Srinivasan, N. A. Yee, E. Agustin, A. Koliszak, E. Miller, I. Khan, I. Quinones, H. Noory, C. Motola, R. Volkmer, M. D. Luca, A. Trampuz, M. Royzen and J. M. M. Oneto, Bio-Orthogonal Chemistry and Reloadable Biomaterial Enable Local Activation of Antibiotic Prodrugs and Enhance Treatments against *Staphylococcus aureus* Infections, *ACS Cent. Sci.*, 2018, **4**, 1624–1632.

33 K. Wu, N. A. Yee, S. Srinivasan, A. Mahmoodi, M. Zakharian, J. M. M. Oneto and M. Royzen, Click activated prodrugs against cancer increase the therapeutic potential of chemotherapy through local capture and activation, *Chem. Sci.*, 2021, **12**, 1259–1271.

34 M. Chang, Y. Dong, H. Xu, A. B. Cruickshank-Taylor, J. S. Kozora, B. Behpour and W. Wang, Senolysis Enabled by Senescent Cell-Sensitive Bioorthogonal Tetrazine Ligation, *Angew. Chem., Int. Ed.*, 2024, **63**, e202315425.

35 N. A. M. Ligthart, M. A. R. de Geus, M. A. T. van de Plassche, D. Torres García, M. M. E. Isendoorn, L. Reinalda, D. Ofman, T. van Leeuwen and S. I. van Kasteren, A Lysosome-Targeted Tetrazine for Organelle-Specific Click-to-Release Chemistry in Antigen Presenting Cells, *J. Am. Chem. Soc.*, 2023, **145**, 12630–12640.

36 W. A. Denny, Tumor-activated Prodrugs—A New Approach to Cancer Therapy, *Cancer Invest.*, 2004, **22**, 604–619.

37 F. Martínez-Jiménez, F. Muñoz, I. Sentís, J. Deu-Pons, I. Reyes-Salazar, C. Arnedo-Pac, L. Mularoni, O. Pich, J. Bonet, H. Kranas, A. Gonzalez-Perez and N. Lopez-Bigas, A compendium of mutational cancer driver genes, *Nat. Rev. Cancer*, 2020, **20**, 555–572.

38 R. Yaeger, R. Mezzadra, J. Sinopoli, Y. Bian, M. Marasco, E. Kaplun, Y. Gao, H. Zhao, A. D. C. Paula, Y. Zhu, A. C. Perez, K. Chadalavada, E. Tse, S. Chowdhry, S. Bowker, Q. Chang, B. Qeriqi, B. Weigelt, G. J. Nanjangud, M. F. Berger, H. Der-Torossian, K. Anderes, N. D. Soccia, J. Shia, G. J. Riely, Y. R. Murciano-Goroff, B. T. Li, J. G. Christensen, J. S. Reis-Filho, D. B. Solit, E. d. Stanchina, S. W. Lowe, N. Rosen and S. Misale, Molecular characterization of acquired resistance to KRAS G12C-EGFR inhibition in colorectal cancer, *Cancer Discovery*, 2022, **13**, 41–55.

39 X. Li, J. Ye, J. Wang, Z. Quan, G. Li, W. Ma, M. Zhang, W. Yang, J. Wang, T. Ma, F. Kang and J. Wang, First-in-Humans PET Imaging of KRASG12C Mutation Status in Non-Small Cell Lung and Colorectal Cancer Patients Using ¹⁸F PFPMD, *J. Nucl. Med.*, 2023, **64**, 1880–1888.

40 X. Sun, Z. Xiao, G. Chen, Z. Han, Y. Liu, C. Zhang, Y. Sun, Y. Song, K. Wang, F. Fang, X. Wang, Y. Lin, L. Xu, L. Shao, J. Li,



Z. Cheng, S. S. Gambhir and B. Shen, A PET imaging approach for determining EGFR mutation status for improved lung cancer patient management, *Sci. Transl. Med.*, 2018, **10**, eaan8840.

41 P. A. Morese, N. Anthony, M. Bodnarchuk, C. Jennings, M. P. Martin, R. A. Noble, N. Phillips, H. D. Thomas, L. Z. Wang, A. Lister, M. E. M. Noble, R. A. Ward, S. R. Wedge, H. L. Stewart and M. J. Waring, Targeting Cytotoxic Agents through EGFR-Mediated Covalent Binding and Release, *J. Med. Chem.*, 2023, **66**(17), 12324–12341.

42 R. N. Reddi, A. Rogel, R. Gabizon, D. G. Rawale, B. Harish, S. Marom, B. Tivon, Y. S. Arbel, N. Gurwicz, R. Oren, K. David, J. Liu, S. Duberstein, M. Itkin, S. Malitsky, H. Barr, B.-Z. Katz, Y. Herishanu, I. Shachar, Z. Shulman and N. London, Sulfamate Acetamides as Self-Immobilative Electrophiles for Covalent Ligand-Directed Release Chemistry, *J. Am. Chem. Soc.*, 2023, **145**, 3346–3360.

43 R. N. Reddi, A. Rogel, E. Resnick, R. Gabizon, P. K. Prasad, N. Gurwicz, H. Barr, Z. Shulman and N. London, Site-Specific Labeling of Endogenous Proteins Using CoLDR Chemistry, *J. Am. Chem. Soc.*, 2021, **143**, 20095–20108.

44 R. N. Reddi, E. Resnick, A. Rogel, B. V. Rao, R. Gabizon, K. Goldenberg, N. Gurwicz, D. Zaidman, A. Plotnikov, H. Barr, Z. Shulman and N. London, Tunable Methacrylamides for Covalent Ligand Directed Release Chemistry, *J. Am. Chem. Soc.*, 2021, **143**, 4979–4992.

45 C. L. Arteaga and J. A. Engelman, ERBB Receptors: From Oncogene Discovery to Basic Science to Mechanism-Based Cancer Therapeutics, *Cancer Cell*, 2014, **25**, 282–303.

46 R. Roskoski, Properties of FDA-approved small molecule protein kinase inhibitors: A 2024 update, *Pharmacol. Res.*, 2024, **200**, 107059.

47 D. Li, L. Ambrogio, T. Shimamura, S. Kubo, M. Takahashi, L. R. Chirieac, R. F. Padera, G. I. Shapiro, A. Baum, F. Himmelsbach, W. J. Rettig, M. Meyerson, F. Solca, H. Greulich and K. K. Wong, BIBW2992, an irreversible EGFR/HER2 inhibitor highly effective in preclinical lung cancer models, *Oncogene*, 2008, **27**, 4702–4711.

48 R. T. Dungo and G. M. Keating, Afatinib: First Global Approval, *Drugs*, 2013, **73**, 1503–1515.

49 F. Solca, G. Dahl, A. Zoepf, G. Bader, M. Sanderson, C. Klein, O. Kraemer, F. Himmelsbach, E. Haaksma and G. R. Adolf, Target Binding Properties and Cellular Activity of Afatinib (BIBW 2992), an Irreversible ErbB Family Blocker, *J. Pharmacol. Exp. Ther.*, 2012, **343**, 342–350.

50 S. Liu, W. Song, X. Gao, Y. Su, E. Gao and Q. Gao, Discovery of Nonpeptide, Reversible HER1/HER2 Dual-Targeting Small-Molecule Inhibitors as Near-Infrared Fluorescent Probes for Efficient Tumor Detection, Diagnostic Imaging, and Drug Screening, *Anal. Chem.*, 2019, **91**, 1507–1515.

51 G. M. Burslem, B. E. Smith, A. C. Lai, S. Jaime-Figueroa, D. C. McQuaid, D. P. Bondeson, M. Toure, H. Dong, Y. Qian, J. Wang, A. P. Crew, J. Hines and C. M. Crews, The Advantages of Targeted Protein Degradation Over Inhibition: An RTK Case Study, *Cell Chem. Biol.*, 2018, **25**, 67–77 e63.

52 B. L. Oliveira, Z. Guo and G. J. L. Bernardes, Inverse electron demand Diels–Alder reactions in chemical biology, *Chem. Soc. Rev.*, 2017, **46**, 4895–4950.

53 J. M. McFarland, M. a. Alečković, G. Coricor, S. Srinivasan, M. Tso, J. Lee, T.-H. Nguyen and J. M. M. a. Oneto, Click Chemistry Selectively Activates an Auristatin Prodrug with either Intratumoral or Systemic Tumor-Targeting Agents, *ACS Cent. Sci.*, 2023, **9**, 1400–1408.

54 G. T. Merlini, Y.-H. Xu, S. Ishii, A. J. L. Clark, K. Semba, K. Toyoshima, T. Yamamoto and I. Pastan, Amplification and Enhanced Expression of the Epidermal Growth Factor Receptor Gene in A431 Human Carcinoma Cells, *Science*, 1984, **224**, 417–419.

55 S. Sritharan and N. Sivalingam, A comprehensive review on time-tested anticancer drug doxorubicin, *Life Sci.*, 2021, **278**, 119527.

56 P. Schöffski, J.-P. Delord, E. Brain, J. Robert, H. Dumez, J. Gasmi and A. Trouet, First-in-man phase I study assessing the safety and pharmacokinetics of a 1-hour intravenous infusion of the doxorubicin prodrug DTS-201 every 3 weeks in patients with advanced or metastatic solid tumours, *Eur. J. Cancer*, 2017, **86**, 240–247.

57 R. Rossin, S. M. J. van Duijnhoven, W. ten Hoeve, H. M. Janssen, L. H. J. Kleijn, F. J. M. Hoeben, R. M. Versteegen and M. S. Robillard, Triggered Drug Release from an Antibody–Drug Conjugate Using Fast “Click-to-Release” Chemistry in Mice, *Bioconjugate Chem.*, 2016, **27**, 1697–1706.

58 I. Khan, P. F. Agris, M. V. Yigit and M. Royzen, In situ activation of a doxorubicin prodrug using imaging-capable nanoparticles, *Chem. Commun.*, 2016, **52**, 6174–6177.

59 R. L. Bai, G. R. Pettit and E. Hamel, Binding of dolastatin 10 to tubulin at a distinct site for peptide antimitotic agents near the exchangeable nucleotide and vinca alkaloid sites, *J. Biol. Chem.*, 1990, **265**, 17141–17149.

60 A. Younes, U. Yasothan and P. Kirkpatrick, Brentuximab vedotin, *Nat. Rev. Drug Discovery*, 2012, **11**, 19–20.

61 S. Gnaim, A. Scomparin, S. Das, R. Blau, R. Satchi-Fainaro and D. Shabat, Direct Real-Time Monitoring of Prodrug Activation by Chemiluminescence, *Angew. Chem., Int. Ed.*, 2018, **57**, 9033–9037.

62 M. Handula, K.-T. Chen and Y. Seimblle, IEDDA: An Attractive Bioorthogonal Reaction for Biomedical Applications, *Molecules*, 2021, **26**, 4640.

63 J. J. Gruskos, G. Zhang and D. Buccella, Visualizing Compartmentalized Cellular Mg²⁺ on Demand with Small-Molecule Fluorescent Sensors, *J. Am. Chem. Soc.*, 2016, **138**, 14639–14649.

64 L. Wang, M. Tran, E. D'Este, J. Roberti, B. Koch, L. Xue and K. Johnsson, A general strategy to develop cell permeable and fluorogenic probes for multicolour nanoscopy, *Nat. Chem.*, 2020, **12**, 165–172.

65 E. Kozma, I. Nikić, B. R. Varga, I. V. Aramburu, J. H. Kang, O. T. Fackler, E. A. Lemke and P. Kele, Hydrophilic trans-Cyclooctenylated Noncanonical Amino Acids for Fast Intracellular Protein Labeling, *ChemBioChem*, 2016, **17**, 1518–1524.



66 H.-J. Chen, C. Y. Chew, E.-H. Chang, Y.-W. Tu, L.-Y. Wei, B.-H. Wu, C.-H. Chen, Y.-T. Yang, S.-C. Huang, J.-K. Chen, I. C. Chen and K.-T. Tan, S-Cis Diene Conformation: A New Bathochromic Shift Strategy for Near-Infrared Fluorescence Switchable Dye and the Imaging Applications, *J. Am. Chem. Soc.*, 2018, **140**, 5224–5234.

67 J. E. Pigga, J. E. Rosenberger, A. Jemas, S. J. Boyd, O. Dmitrenko, Y. Xie and J. M. Fox, General, Divergent Platform for Diastereoselective Synthesis of trans-Cyclooctenes with High Reactivity and Favorable Physicochemical Properties, *Angew. Chem., Int. Ed.*, 2021, **60**, 14975–14980.

68 M. Srinivasarao, C. V. Galliford and P. S. Low, Principles in the design of ligand-targeted cancer therapeutics and imaging agents, *Nat. Rev. Drug Discovery*, 2015, **14**, 203–219.

69 W. Kuba, B. Sohr, P. Keppel, D. Svatunek, V. Humhal, B. Stöger, M. Goldeck, J. C. T. Carlson and H. Mikula, Oxidative Desymmetrization Enables the Concise Synthesis of a trans-Cyclooctene Linker for Bioorthogonal Bond Cleavage, *Chem. - Eur. J.*, 2023, **29**, e202203069.

70 J. M. McFarland, M. Alečković, G. Coricor, S. Srinivasan, M. Tso, J. Lee, T.-H. Nguyen and J. M. Mejía Oneto, Click Chemistry Selectively Activates an Auristatin Prodrug with either Intratumoral or Systemic Tumor-Targeting Agents, *ACS Cent. Sci.*, 2023, **9**, 1400–1408.

71 X. Xu, Y. Wang, Y. Shi, X. Wang, X. Tong, Y. Chen, Y. Zhao, J. Chen, W. Guo and Y. Zheng, Development of Cyclooctyne-Nitrone Based Click Release Chemistry for Bioorthogonal Prodrug Activation both In Vitro and In Vivo, *J. Am. Chem. Soc.*, 2025, **147**, 34425–34437.

72 I. M. Serafimova, M. A. Pufall, S. Krishnan, K. Duda, M. S. Cohen, R. L. Maglathlin, J. M. McFarland, R. M. Miller, M. Frödin and J. Taunton, Reversible targeting of noncatalytic cysteines with chemically tuned electrophiles, *Nat. Chem. Biol.*, 2012, **8**, 471.

73 D. Lu, X. Yu, H. Lin, R. Cheng, E. Y. Monroy, X. Qi, M. C. Wang and J. Wang, Applications of covalent chemistry in targeted protein degradation, *Chem. Soc. Rev.*, 2022, **51**, 9243–9261.

74 H. Kiely-Collins, G. E. Winter and G. J. L. Bernardes, The role of reversible and irreversible covalent chemistry in targeted protein degradation, *Cell Chem. Biol.*, 2021, **28**, 952–968.

75 M. a. Maneiro, N. Forte, M. M. Shchepinova, C. S. Kounde, V. Chudasama, J. R. Baker and E. W. Tate, Antibody-PROTAC Conjugates Enable HER2-Dependent Targeted Protein Degradation of BRD4, *ACS Chem. Biol.*, 2020, **15**, 1306–1312.

76 K. Tsuchikama, Y. Anami, S. Y. Y. Ha and C. M. Yamazaki, Exploring the next generation of antibody-drug conjugates, *Nat. Rev. Clin. Oncol.*, 2024, **21**, 203–223.

77 J. Hallin, L. D. Engstrom, L. Hargis, A. Calinisan, R. Aranda, D. M. Briere, N. Sudhakar, V. Bowcut, B. R. Baer, J. A. Ballard, M. R. Burkard, J. B. Fell, J. P. Fischer, G. P. Vigers, Y. Xue, S. Gatto, J. Fernandez-Banet, A. Pavlicek, K. Velastagui, R. C. Chao, J. Barton, M. Pierobon, E. Baldelli, E. F. Patricoin, D. P. Cassidy, M. A. Marx, I. I. Rybkin, M. L. Johnson, S.-H. I. Ou, P. Lito, K. P. Papadopoulos, P. A. Jänne, P. Olson and J. G. Christensen, The KRAS^{G12C} Inhibitor MRTX849 Provides Insight toward Therapeutic Susceptibility of KRAS-Mutant Cancers in Mouse Models and Patients, *Cancer Discovery*, 2020, **10**(1), 54–71.

78 M. R. Janes, J. Zhang, L.-S. Li, R. Hansen, U. Peters, X. Guo, Y. Chen, A. Babbar, S. J. Firdaus, L. Darjania, J. Feng, J. H. Chen, S. Li, S. Li, Y. O. Long, C. Thach, Y. Liu, A. Zarieh, T. Ely, J. M. Kucharski, L. V. Kessler, T. Wu, K. Yu, Y. Wang, Y. Yao, X. Deng, P. P. Zarrinkar, D. Brehmer, D. Dhanak, M. V. Lorenzi, D. Hu-Lowe, M. P. Patricelli, P. Ren and Y. Liu, Targeting KRAS Mutant Cancers with a Covalent G12C-Specific Inhibitor, *Cell*, 2018, **172**, 578–589. e517.

79 A. Sadagopan, M. Carson, E. J. Zamurs, N. Garaffo, H.-J. Chang, S. L. Schreiber, M. Meyerson and W. J. Gibson, Mutant p53 protein accumulation is selectively targetable by proximity-inducing drugs, *Nat. Chem. Biol.*, 2025, DOI: [10.1038/s41589-025-02051-7](https://doi.org/10.1038/s41589-025-02051-7).

